Sensors & Diagnostics

PAPER

View Article Online
View Journal | View Issue

Cite this: *Sens. Diagn.*, 2024, **3**, 1159

Enhanced spin-polarization and detection limit in a spin-based optoelectrochemical DNA hybridization sensor induced by circularly polarized light†

Mayank Tiwari and Debabrata Mishra *

We investigate the influence of the correlation between different types of polarized light (linear and circular) and spin-polarization $|P_s|$ (in %) on the effectiveness of a spin-based quantum dot-modified DNA device for a DNA hybridization sensor. The device exhibits a significant two-fold increase in $|P_s|$ (in %) when exposed to circularly polarized (C.P.) light, in comparison to the state of no illumination. This improvement in $|P_s|$ results in a significant ten-fold enhancement in the limit of detection (L.O.D.) of the electrode under C.P. light illumination, surpassing the conditions without illumination and even achieving a two-fold increase compared to linearly polarized (L.P.) light illumination. These results emphasize the crucial significance of polarized light in maximizing the efficiency of spin-based DNA hybridization sensors. The significant enhancements in the performance observed under C.P. light illumination demonstrate the potential use of our device to function as a highly sensitive and efficient tool in spin-based bio-sensing applications.

Received 7th April 2024,
Accepted 13th May 2024

DOI: 10.1039/d4sd00109e

rsc.li/sensors

1 Introduction

Electrochemical impedance spectroscopy (EIS) is a precise and dependable method employed in electrochemical DNA biosensing.[1,2] It detects DNA hybridization by measuring impedance changes resulting from DNA binding events.[3] When the specific complementary DNA sequence binds to the probe DNA (ss-DNA) on the electrode, the transducer measures impedance changes at the electrode–electrolyte interface.[4] This alteration in impedance is detected using a low-intensity alternating signal at various frequencies.[5] Nevertheless, conventional EIS methods have inherent drawbacks, such as the existence of perturbations and susceptibility to false signals. These factors can cause a change in impedance even when no hybridization occurs, which directly affects the performance of the biosensor, including its sensitivity and limit of detection (L.O.D.).[6] However, the limitations of conventional EIS can be effectively addressed or overcome with the emergence of the chiral-induced spin selectivity (CISS) effect, facilitating the advancement of spin-based DNA biosensor technology.[7–10]

The CISS effect originates from the interconnection between an electron's spin and the chirality in the structure of a molecule, causing one spin orientation to pass through the molecule, while the opposite spin orientation undergoes backscattering.[11,12] This is observed in structures like amino acids, peptides, and ds-DNA.[11,13,14] Utilizing the spin filtering ability and chirality in the ds-DNA structure, various studies on spin-based DNA sensors have been reported. Recently, Bangruwa *et al.* designed a spin-based DNA hybridization sensor (electrochemical) for dengue virus detection. The group utilized the inherent chirality in the secondary structure of ds-DNA and the spin of the transferred electrons as innovative tools to directly probe hybridization in DNA, achieving a detection limit of 0.12 pM.[7] The same group also fabricated a chiral-induced spin selectivity (CISS)-based impedimetric DNA damage detection sensor with a 10 pM limit of detection (L.O.D.).[8] These spin-based impedimetric DNA hybridization sensors utilize the inherent chirality in the secondary structure of ds-DNA to evaluate the relative charge-transfer resistance (ΔR_{ct}) instead of the overall charge-transfer resistance (R_{ct}) typically measured in a conventional impedimetric device.[7,9] The relative charge-transfer resistance (ΔR_{ct}) is the difference in the charge-transfer resistance calculated for the up and down spins of electrons, which only depends on the spin ability of ds-DNA. This difference in the relative charge-transfer resistance (ΔR_{ct}) results in spin polarization ($|P_s|$%), which directly correlates with important parameters such as selectivity, sensitivity, and L.O.D. in these spin-based biosensors. The most important advantage of spin-

Department of Physics and Astrophysics, University of Delhi, New Delhi 110007, India. E-mail: dmishra@physics.du.ac.in

† Electronic supplementary information (ESI) available. See DOI: https://doi.org/10.1039/d4sd00109e

based DNA detection devices over conventional electrochemical biosensors is their ability to address the issue of false signals by substituting the electronic charge current with the spin-polarized current, also referred to as the CISS-induced current.[7,8] The spin-polarized current is not influenced by external perturbations and is exclusively determined by the inherent structural symmetry of the molecule for its control.[15,16] Any change in the inherent structure of the molecule directly influences the spin-polarized current and the change is verified.[15,16] Bangruwa *et al.* explored the effect of point mutation and changing sequence on spin polarization in a spin-based DNA/QD device. A change in the sequence was directly correlated with the spin polarization in the QD DNA system.[15] Moreover, these spin-based devices employ spin-polarization values as a criterion for distinguishing instead of traditional current or charge transfer resistance values.[7,15,16] This approach directly corresponds to the intrinsic structure of the molecules being studied, rather than depending merely on their electrical properties. To enhance the performance of spin-based DNA biosensors, it is thus crucial to enhance the spin polarization ($|P_s|$%) and correlate its value with the biosensor's parameters.

It is well-established that light can excite electrons in a variety of materials, including metals, semiconductors, quantum dots, *etc.*[17,18] Additionally, the orientation of the light's electric and magnetic field vectors can selectively stimulate electrons with specific spin orientations.[19,20] This stimulation influences spin dynamics and facilitates the generation of spin-polarized currents, thereby impacting the spin polarization of the system under study. Abendroth *et al.* investigated the impact of light on the quantum dot–DNA (QD-DNA) system assembled on a ferromagnetic substrate and observed a variation in the fluorescence intensity corresponding to the up and down spins of the electrons.[21] Ray *et al.* experimentally demonstrated the role of linearly and circularly polarized light in generating spin polarization in L and D-stearoyl lysine monolayers.[22] Recently, Bhartiya *et al.* developed a QD/DNA impedimetric device and demonstrated an enhancement in spin polarization with light stimulation, resulting in increased sensitivity and a lower limit of detection (L.O.D.) for the device.[9] These findings highlight the significant impact of light on spin polarization, which has great potential to optimize the efficiency and performance of spin-based devices. Furthermore, it is crucial to recognize the specific impacts of linearly and circularly polarized light on spin-polarization for upgrading the functionalities of these devices and improving their practical use in spin-based biosensors.

In light of these findings, we develop a spin-based opto-electrochemical impedimetric device by assembling DNA monolayers on Co_2FeAl (CFA) thin films. Utilizing Co_2FeAl (a ferromagnetic Heusler alloy) for spin injection, we incorporated core–shell CdSe/ZnS quantum dots (QDs) in the devices for the photo-excitation of electrons. We correlated the role of polarization of light (linear and circular) and spin-polarization ($|P_s|$%) of the system with the performance of the CFA/DNA/QD device utilized as a DNA hybridization sensor.

2 Materials and methods

2.1 Materials

Necessary chemicals potassium hexacyanoferrate(III) [K_3-$Fe(CN)_6$] and potassium hexacyanoferrate(II) trihydrate [K_3-$Fe(CN)_6{\cdot}3H_2O$] were purchased from Sigma Aldrich. Other chemicals such as DNA sequences, core–shell CdSe/ZnS quantum dots, and Cr were purchased from Sigma Aldrich. In addition, high-purity (99.99%) gold (Au) wire was procured from Beeta Tech India.

2.2 Fabrication of Co_2FeAl (CFA) thin films

Ferromagnetic CFA thin films with gold (Au) overlayers were utilized as the electrode platform for the self-assembly of DNA monolayers. The CFA thin films with Au overlayer electrode platforms were fabricated using the physical vapor deposition (PVD) technique. For this, a 100 nm layer of CFA was deposited onto a glass substrate using the electron beam evaporation technique. To promote bonding between the CFA thin film and the glass substrate, a 5 nm binding layer of chromium was deposited using thermal evaporation. Au patches with circular patterns were created on the CFA by using a shadow mask during the deposition process of 10 nm Au. The deposition process was conducted at a precisely regulated rate of 0.2 Å s^{-1} in a high vacuum environment with a pressure of 10^{-7} Torr. Fig. 2(a) presents the image of the CFA thin film with circular patterns of Au formed after utilizing the shadow mask during the deposition process.

2.3 Preparation of self-assembled monolayers (SAMs) of DNA on CFA thin films

Following the fabrication process of the CFA thin films coated with an Au layer, self-assembled monolayers (SAMs) of DNA were attached to the Au-coated CFA thin films. The CFA thin film was first subjected to a cleaning procedure, which involved immersing it in acetone and ethanol (15 minutes) and drying it using nitrogen gas. Furthermore, the thin film was subjected to UV radiation to eradicate any potential organic contamination. Afterwards, the film was swiftly purified using ethanol and subsequently dried with nitrogen gas. 10 μM primer or the single-stranded DNA (ss-DNA), modified with amide and thiol groups, was immobilized onto the CFA thin film using the drop-casting method.[10] Subsequently, it was subjected to a wet environment for 24 hours to facilitate the immobilization of self-assembled monolayers (SAMs) of the ssDNA. To affix core–shell CdSe/ZnS quantum dots (QDs) onto the SAMs of the ss-DNA, a toluene solution of CdSe/ZnS core–shell quantum dots (0.5 μM) was formed. The solution was applied to the SAMs of the single-stranded DNA (ss-DNA) and allowed to undergo a reaction for four hours in the absence of light. During this time, quantum dots (QDs) were linked with the amide group that was linked to one end of the ss-DNA. Following that time

Table 1 Sequences of oligonucleotides used in this work

Type of DNA	Sequence
Primer	5′-NH_2-GACCACAGATTCAAACATGCGACCACAGATTCAA-ACATGC-($ThiC_3$)-3′
Complementary	3′-CTGGTGTCTAAGTTTGTACGCTGGTGTCTAAGTTTGTACG-5′
Non-complementary	5′-GAGCAGAGATTCAAACATGCGACCACAGATTCAAACATGC-3′

frame, the SAMs containing quantum dots (QDs) bound to DNA were cleansed using toluene and dried using nitrogen gas to eliminate any unbound QDs. This process led to the creation of a monolayer system consisting of QD-attached single-stranded DNA (CFA/ss-DNA/QD). To promote the formation of monolayers composed of double-stranded DNA (ds-DNA) and non-complementary DNA (nc-DNA), the self-assembled monolayers (SAMs) of quantum dot-single-stranded DNA on the CFA thin film (CFA/ss-DNA/QD) were hybridized with the complementary and non-complementary sequences using standard protocols.[20] The primer DNA sequences form hydrogen bonds with their complementary DNA sequences, forming a double-stranded helix. The CFA thin films with ds-DNA and QDs were abbreviated as CFA/ds-DNA/QD. The QD-attached non-complementary sequence on the CFA thin film was abbreviated as CFA/nc-DNA/QD. The DNA sequences used in the experiment are provided in Table 1.

2.4 Optical setup for linearly polarized (L.P.) and circularly polarized (C.P.) light

The optical arrangement part shown in Fig. 1 was used to generate L.P. and C.P. light. For this, a laser light source emitting at a wavelength of 532 nm was utilized, along with polarizers and a quarter-wave plate. To obtain linear polarization, the laser light was allowed to pass through a linear polarizer. Furthermore, C.P. light was produced by passing the L.P. light from the linear polarizer through a quarter-wave plate, positioned at a 45-degree angle to the polarizer's orientation.

2.5 Characterization

The structural and crystallographic characterization of the deposited CFA thin films with Au overlayers was achieved by the X-ray diffraction (XRD) technique by utilizing a Rigaku Ultima IV X-ray diffractometer (Cu source with a wavelength (λ) of 1.54 nm). A NICOLET iS50 Fourier transform-infrared (FT-IR) spectrophotometer was utilized to capture the distinctive FT-IR spectra of the CdSe/ZnS (QD)-attached SAMs of DNA assembled on the CFA thin films. A two-electrode electrochemical setup connected to an electrochemical workstation (CORRTEST CS350 model) along with the optical arrangement (described in section 2.4 and Fig. 1) was utilized for conducting all spin-dependent electrochemical studies, which included electrochemical impedance spectroscopy (EIS).

3 Results and discussion

3.1 Characterization of the CFA/DNA/QD device

The crystallographic morphology of the CFA thin film was characterized by the X-ray diffraction (XRD) method. For this,

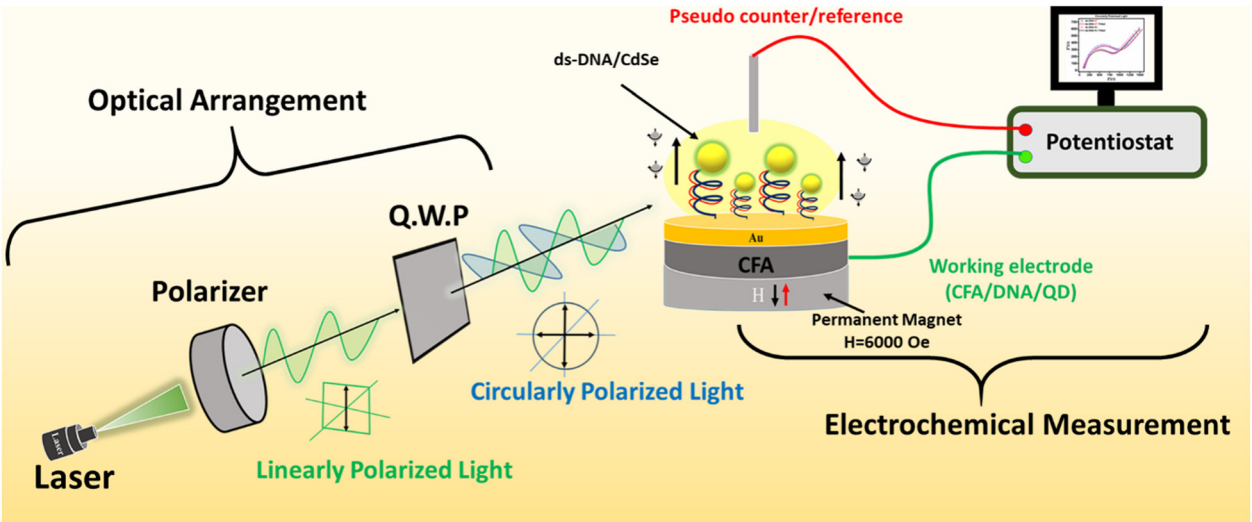

Fig. 1 Schematic illustration of the experimental arrangement for light-enabled spin-based DNA biosensing on the CFA/DNA/QD assembly comprising two main setups. The optical arrangement setup includes a linear polarizer and a quarter wave plate to generate L.P. and C.P. light, respectively. Concurrently, the electrochemical measurement setup features a CFA thin film with an Au overlayer. Core–shell CdSe/ZnS quantum dot (QD)-attached self-assembled monolayers (SAMs) of DNA are assembled on this thin film in a two-electrode configuration, with Pt serving as a pseudo-counter/reference electrode, all connected to a potentiostat for electrochemical impedance analysis. The electrochemical impedance measurements were performed by using 2 μL of 5 mM $K_4Fe(CN)_6/K_3Fe(CN)_6$ in a pH 7.2 phosphate buffer solution as the electrolyte.

CFA was deposited on the silicon substrate and XRD was performed. Fig. 2(b) presents the XRD pattern of the CFA thin film. The peak at around 32.5° represents the (0 0 2) plane[23] and the peak observed at around 44.5° corresponds to the (2 2 0) plane.[24] The XRD pattern confirms the presence of the (*h k l*) planes of CFA without any extra peak and impurity. The formation of QD-attached DNA monolayers on the CFA thin films was confirmed by the FT-IR spectroscopy technique. Fig. 2(c) and (d) present the different vibrational peaks observed in the FT-IR spectra of the CFA/ss-DNA/QD and CFA/ds-DNA/QD devices, respectively. Peak number 1 observed at around 1070 cm^{-1} for the CFA/ss-DNA/QD and CFA/ds-DNA/QD devices represents the CO stretching.[10,25] Peaks observed at around 1114 cm^{-1} and 1270 cm^{-1} (marked as 2) both represent the asymmetric and symmetric groups belonging to the phosphodiester backbone (PO_4^- group).[10,25] The C4C5 vibrations at 1470 cm^{-1} are represented by peak 3. Peak 4 at around 1580 cm^{-1} in Fig. 2(d) represents the in-phase guanine vibration. Furthermore, the vibrational frequency at 1675 cm^{-1} confirms the base pairing of guanine C6═O6.[7,25] The presence of more pronounced and additional peaks in the vibrational spectrum of CFA/ds-DNA/QD confirms the formation of double-stranded DNA, indicating the creation of new bonds following the hybridization process.

3.2 Light-enabled spin-based electrochemical impedance spectroscopy (EIS)

To investigate the role of linearly and circularly polarized light in the spin polarization of the electrodes, the spin-based EIS technique was performed using a two-electrode setup on the CFA/DNA/QD devices first in the absence and then in the presence of a laser light source at a wavelength of 532 nm and a magnetic field strength of 6000 Oe.[7,9] Fig. 1 illustrates the schematics of the experimental setup utilized to perform light-enabled CISS-based EIS. CFA/ss-DNA/QD, CFA/ds-DNA/QD, and CFA/nc-DNA/QD were used as the working electrodes, Pt wire as the reference/counter electrode, and phosphate buffer solution (2 L) with a redox couple (Fe^{3+}/Fe^{2+}) was used as the electrolyte. A magnetic field with a strength of 6000 Oe was used for up ($H\uparrow$) and down ($H\downarrow$) spin injection by polarizing the ferromagnetic CFA thin film.

3.2.1 Spin-based EIS in the absence of light. Spin-based EIS measurements were performed on each CFA/DNA/QD device at a 10 mV amplitude and 10^5 to 10^0 Hz frequency range. A magnetic field with a strength of H = 6000 Oe was placed beneath the CFA/DNA/QD electrode during the measurement to inject spin-up ($H\uparrow$) and spin-down ($H\downarrow$) electrons through the ferromagnetic CFA thin film. Fig. 3 presents the Nyquist plots of the CFA/DNA/QD devices in the absence of any illumination with a laser light source (no light). Fig. 3(a) presents the Nyquist plot of the CFA/ss-DNA/QD device for spin-up ($H\uparrow$) and spin-down ($H\downarrow$) EIS measurements. The Nyquist plot was fitted utilizing EIS-analyzer software, and the value of the spin-based charge transfer resistance (R_{ct}) was calculated by measuring the diameter of the semicircle in the Nyquist plot for spin-up and spin-down electrons represented by $R_{ct\uparrow}$ and $R_{ct\downarrow}$, respectively. Using the R_{ct} values, the spin polarization ($|P_s|$%) was calculated for the CFA/ss-DNA/QD device in the absence of light using the equation:[15]

$$|P_s| = \frac{R_{ct\downarrow} - R_{ct\uparrow}}{R_{ct\downarrow} + R_{ct\uparrow}} \times 100. \quad (1)$$

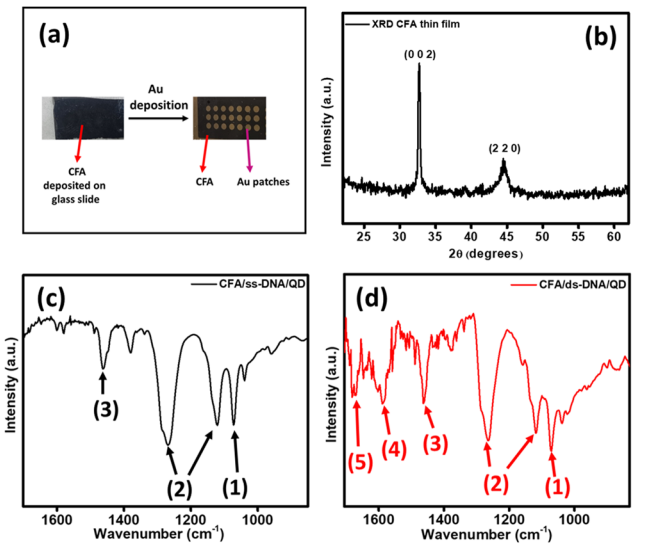

Fig. 2 (a) Real image of the CFA thin film with gold overlayers deposited by the PVD technique. Circular Au patterns were created on the CFA thin film using a shadow mask during the deposition process. (b) XRD pattern of the CFA thin film. FT-IR spectra of the QD-attached SAMs with (c) ss-DNA and (d) ds-DNA on the CFA thin film device.

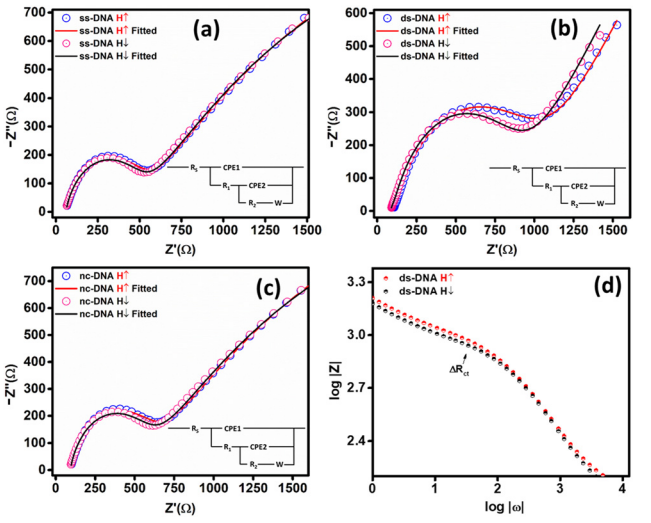

Fig. 3 Nyquist plots (electrochemical impedance spectroscopy (EIS)) for (a) CFA/ss-DNA/QD, (b) CFA/ds-DNA/QD (after hybridization with the complementary sequence), and (c) CFA/nc-DNA/QD devices. (d) EIS Bode magnitude plot for CFA/ds-DNA/QD (all the measurements are performed in the absence of any illumination in a two-electrode setup).

The spin polarization for CFA/ss-DNA/QD was found to be 0% in the absence of light. The ss-DNA was then hybridized with the complementary and non-complementary sequences to form CFA/ds-DNA/QD and CFA/nc-DNA/QD. CISS-based EIS measurements were again performed on the CFA/ds-DNA/QD and CFA/nc-DNA/QD devices.

Fig. 3(b) presents the fitted Nyquist plot for CFA/ds-DNA/QD. The charge transfer resistance (R_{ct}) was calculated by measuring the diameter of the semicircle in the Nyquist plot. A change in the R_{ct} is observed for the ds-DNA device for spin-down electrons. Spin-polarization was calculated using eqn (1) and was found to be 5.0 ± 0.3%. For the nc-DNA, the spin polarization was calculated from the Nyquist plot in Fig. 3(c) and was found to be 0%. The helix of the ds-DNA allows spin-down electrons to pass easily due to the CISS effect, resulting in a lower R_{ct} value for spin-down electrons and a higher R_{ct} value for spin-up electrons. However, when hybridized with the non-complementary sequence, the CISS effect is again negligible resulting in hybridization detection. The highest spin polarization in the absence of any illumination was observed to be 5.0% for CFA/ds-DNA/QD, *i.e.* when the ss-DNA was hybridized with the complementary sequence. Fig. 3(d) presents the Bode plot of the CFA/ds-DNA/QD device for spin-up and down measurements.

3.2.2 Spin-based EIS under linearly polarized (L.P.) light. The impact of L.P. light on the spin polarization was observed for the CFA/ss-DNA/QD, CFA/ds-DNA/QD, and CFA/nc-DNA/QD devices. For this, spin-based EIS was performed as in section 3.2.1 by illuminating the electrodes with an L.P. light source with a wavelength of 532 nm. The L.P. light source was formed by placing a polarizer in front of the laser light source. Fig. 4 illustrates the fitted Nyquist plot for EIS measurement under an L.P. light source. The spin polarization was calculated for the CFA/ss-DNA/QD, CFA/ds-DNA/QD, and CFA/nc-DNA/QD devices under the influence of the L.P. light source. No change in the value of spin polarization was observed for ss-DNA and nc-DNA as shown in Fig. 4(a) and (c). However, the spin polarization was increased from 5.0 ± 0.3% to 6.5 ± 0.3% when the CFA/ds-DNA/QD device was illuminated with L.P. light. The change in R_{ct} is also seen in the Bode plot of the CFA/ds-DNA/QD device under L.P. light (see Fig. 4(d)). The application of L.P. light slightly intensifies the CISS effect in the ds-DNA–QD device, resulting in a greater spin polarization when compared with the spin polarization measurement under no illumination.

3.2.3 Spin-based EIS under circularly polarized (C.P.) light. The L.P. light from the polarizer was converted to C.P. light by placing a quarter wave plate (Q.W.P.) in front of the polarizer with the axis aligned at 45° with respect to the polarizer's axis. L.P. light passing through the Q.W.P. is converted to C.P. light. The formation of C.P. light was verified by placing an analyzer (with its axis aligned with the Q.W.P.) in front of the quarter wave plate and rotating it. No change in the intensity was observed after rotating the analyzer, thus confirming the formation of a C.P. light source. Spin-based EIS measurements were then performed on the CFA/ss-DNA/QD, CFA/ds-DNA/QD, and CFA/nc-DNA/QD devices in the presence of the C.P. light. Fig. 5(a)–(c) present the fitted Nyquist plots obtained after performing the spin-based EIS measurements on the CFA/ss-DNA/QD, CFA/ds-DNA/QD, and CFA/nc-DNA/QD devices under C.P. light. A remarkable increase in spin-polarization was obtained in the ds-DNA-coated electrode (CFA/ds-DNA/QD). The spin polarization was calculated to be 9.6 ± 0.4% in the presence of C.P. light. There was a remarkable two-fold enhancement in the spin polarization of CFA/ds-DNA/DNA when exposed to circularly polarized (CP) light, and a 1.5 times

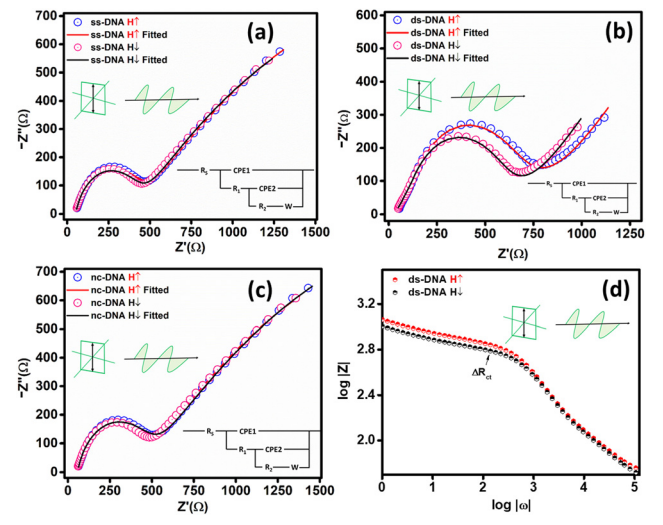

Fig. 4 Nyquist plots (EIS) for (a) CFA/ss-DNA/QD, (b) CFA/ds-DNA/QD (after hybridization with the complementary sequence), and (c) CFA/nc-DNA/QD devices. (d) EIS Bode magnitude plot for CFA/ds-DNA/QD (all the measurements are performed by illuminating the device with L.P. light).

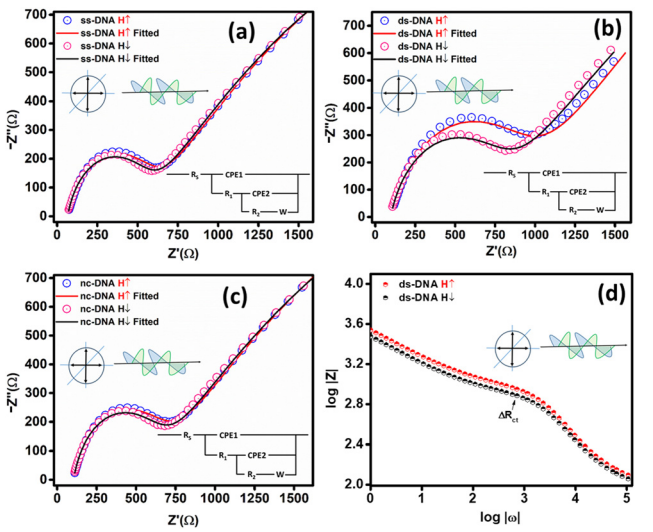

Fig. 5 Nyquist plots (EIS) for (a) CFA/ss-DNA/QD, (b) CFA/ds-DNA/QD (after hybridization with the complementary sequence), and (c) CFA/nc-DNA/QD devices under C.P. light illumination. (d) EIS Bode magnitude plot for CFA/ds-DNA/QD (all the measurements are performed by illuminating the device with C.P. light).

enhancement compared to linearly polarized light. Fig. 5(d) presents the Bode plot showing the difference in the R_{ct} values at different frequencies.

3.3 Role of L.P. and C.P. light in spin-based EIS

Fig. 6(a) depicts the possible scenario leading to high spin polarization in the CFA/ds-DNA/QD devices under C.P. light illumination. When the circularly polarized light (C.P. light) is incident towards the CFA/ds-DNA/QD system (as shown in Fig. 6(a-i)), it stimulates the electronic spin states of the CdSe/ZnS quantum dot (QD) and generates spin-polarized electron–hole pairs in the system (as depicted in Fig. 6(a-ii)).[10] As a result, to balance the charge and spin density of states generated in the system, electrons migrate from the CFA thin film towards the counter electrode *via* the ds-DNA bridge (as depicted in Fig. 6(a-iii)). Nevertheless, the secondary structure of ds-DNA exhibits chirality, which selectively permits a specific spin to pass through it (CISS effect). Consequently, the chirality of ds-DNA facilitates the efficient movement of spin-down electrons (in this case), resulting in a reduced R_{ct} and hindering the migration of spin-up electrons.[10,19] Therefore, a variation in the charge transfer resistance for spin-up and spin-down electrons is observed, which results in the enhancement of spin-polarization under the C.P. light illumination. Nevertheless, when the CFA/ds-DNA/QD device is exposed to linearly polarized (L.P.) light, there is a slight increase in the spin polarization value compared to when there is no illumination. However, this enhancement is not substantial. This is because linearly polarized light does not generate spin-polarized electrons in the system and therefore does not significantly contribute to the enhancement of spin polarization. Fig. 6(b) depicts the spin polarization values ($|P_s|$%) obtained from the Nyquist plots for the CFA/ds-DNA/QD devices in the absence of light and the presence of L.P. and C.P. light.

3.4 Efficacy of the CFA/DNA/QD device as a DNA hybridization sensor under L.P. and C.P. light conditions

To evaluate the device's capability as a biosensor, the spin-polarization was evaluated at different target concentrations (complementary DNA). For this, the probe CFA/ss-DNA/QD system was hybridized with different concentrations of the

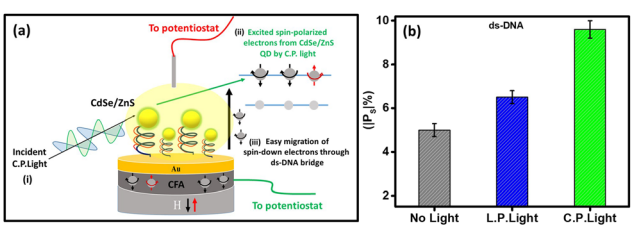

Fig. 6 (a) Schematic illustration of the possible scenario leading to the enhancement in the spin-polarization in the CFA/ds-DNA/QD device under C.P. light illumination. (b) Comparison of the spin-polarization ($|P_s|$ in %) values calculated by multiple measurements on the CFA/ds-DNA/QD devices in the absence and the presence of L.P. and C.P. light.

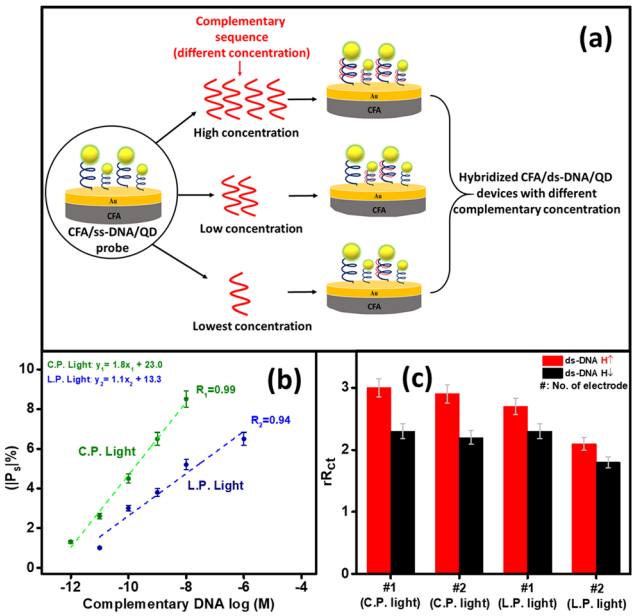

Fig. 7 (a) Schematic illustration of the procedure to check the efficacy of the CFA/DNA/QD device as a biosensor under polarized light illumination. Multiple CFA/ss-DNA/QD (probe) devices were fabricated and hybridized with different complementary sequences resulting in the hybridized CFA/ds-DNA/QD devices with low to high concentrations of the complementary sequences. (b) Fitted $|P_s|$% *vs.* log|*M*| curve after performing EIS on the devices with different concentrations of the complementary DNA under L.P. (highlighted in blue) and C.P. light (highlighted in green) illumination. (c) Reproducibility assessment of the device under L.P. and C.P. light illumination.

complementary sequences as depicted in Fig. 7(a). Spin-based EIS was then performed on the devices with different concentrations of the complementary sequence under L.P. and C.P. light conditions. Fig. 7(b) exhibits the graph of the spin polarization ($|P_s|$%) of the device at different logarithmic target concentrations under L.P. and C.P. light illumination. The device exhibited a linear response in the spin polarization measured at different target concentrations. The graph of $|P_s|$% *vs.* log|*M*| was fitted and the values of the slope and standard error σ were calculated for L.P. and C.P. light. The device's limit of detection (L.O.D.) was measured under the IUPAC guidelines using the formula 3σ/slope for various polarization settings (L.P. and C.P. light conditions).[26,27] When exposed to circularly polarized light, the limit of detection (L.O.D.) was measured to be 0.09 pM, while under linearly polarized light, the L.O.D. was determined to be 0.28 pM. Significantly, the device showed significant enhancement in its limit of detection (L.O.D.) when exposed to L.P. and C.P. light. When compared to the dark conditions with a limit of detection (L.O.D.) of 1 pM, the device exhibited a remarkable tenfold enhancement in sensitivity when exposed to circularly polarized light, resulting in an L.O.D. of 0.09 pM. Between L.P. and C.P. light conditions, the device's L.O.D. was enhanced by up to three times under C.P. light conditions compared to L.P. light

Table 2 Comparison of the performance of spin-based electrochemical DNA biosensors

Spin-based electrochemical study	Application	L.O.D. under no illumination	L.O.D. under L.P. light	L.O.D. under C.P. light	References
E.I.S.	UVC-induced DNA damage detection	10 pM	—	—	8
D.P.V.	Dengue virus detection	0.12 pM	—	—	7
E.I.S.	Sequence-specific DNA detection	—	—	—	15
E.I.S.	DNA hybridization	1 pM	0.28 pM	0.09 pM	This work
E.I.S.	DNA hybridization	100 fM	—	—	9

conditions. The selectivity of the CFA/DNA/QD device was demonstrated through experiments with non-complementary sequences, confirming its ability to distinguish between the target and non-complementary sequence. Spin-based EIS measurements were performed for the non-complementary sequence-attached devices (CFA/nc-DNA/QD) under different conditions, such as no light illumination, L.P. light illumination, and C.P. light illumination. The results demonstrated the absence of substantial spin polarization under all conditions, including no-light, L.P. light, and C.P. light, as depicted in Fig. 3(c), 4(c), and 5(c), respectively. These results indicate that the device could distinguish between the complementary and non-complementary sequences. The strong selectivity of the device ensures the accurate detection of suitable target DNA sequences while distinguishing them from different non-complementary sequences. Table 2 demonstrates the comparison of the performance of spin-based electrochemical DNA biosensors. Furthermore, to determine the reproducibility and reliability of the device, two groups of devices were separately tested to ascertain their capacity to consistently detect DNA hybridization in the presence of L.P and C.P. light.[8] Multiple measurements were performed on both electrodes, and the relative charge transfer resistance (rR_{ct}) was calculated for each electrode for spin-up and spin-down electron transfer. The relative charge transfer resistance (rR_{ct}) was calculated using the formula:[8,9]

$$rR_{ct} = \frac{R_{ctDNA} - R_{ctCFA/Au}}{R_{ctCFA/Au}} \quad (2)$$

Herein, the device's response is denoted by rR_{ct}, which represents the disparity in the relative charge transfer resistance between the self-assembled monolayers (SAMs) of double-stranded DNA (ds-DNA) and the uncoated CFA/Au thin film. Fig. 7(c) presents the rR_{ct} for multiple electrodes under C.P. and L.P. light. The results were reliable and reproducible on different electrodes under illumination.

4 Conclusions

In summary, we investigated the impact of light polarization on the performance of the CFA/DNA/QD device as a spin-based opto-electrochemical DNA hybridization sensor. For this, SAMs of DNA were prepared on CFA, and QDs were decorated on top of that. The setup was then tested for DNA hybridization using a spin-dependent electrochemical impedance measurement. When exposed to circularly polarized light, the device showed a significant two-fold increase in the magnitude of $|P_s|$ and a remarkable ten-fold enhancement in the limit of detection (L.O.D.) of the sensor. We also compared the influence of linear and circular polarization on the spin-polarization and efficacy of this CFA/DNA/QD device. A two-fold improvement in device performance was observed when exposed to C.P. light compared to L.P. light. These findings are crucial in understanding the separate effects of linearly and circularly polarized light on spin polarization in these spin-based DNA sensors for enhancing their sensitivity in spin-based biosensing.

Author contributions

M. T.: conceptualization, data curation, analysis, and manuscript writing; D. M.: conceptualization, analysis, and manuscript writing.

Conflicts of interest

There are no conflicts to declare.

Acknowledgements

D. M. acknowledges the financial support from MHRD-DST through Grant No. IMP/2018/001668, SERB through Grant No. CRG/2018/004264, IoE (University of Delhi) through Grant No. IoE/2021/12/FRP, and UGC through Grant No. F.4-5(202-FRP)/2015(BSR). M. T. acknowledges UGC and CSIR New Delhi for providing financial support.

Notes and references

1 I. K. Bigdeli, M. Yeganeh, M. T. Shoushtari and M. K. Zadeh, *Nanosensors for Smart Manufacturing*, Elsevier, 2021, pp. 533–554.
2 X. Liu, X. Qu, J. Dong, S. Ai and R. Han, *Biosens. Bioelectron.*, 2011, **26**, 3679–3682.
3 D. Li, X. Zou, Q. Shen and S. Dong, *Electrochem. Commun.*, 2007, **9**, 191–196.
4 V. Freger and S. Bason, *J. Membr. Sci.*, 2007, **302**, 1–9.
5 A. Li, F. Yang, Y. Ma and X. Yang, *Biosens. Bioelectron.*, 2007, **22**, 1716–1722.
6 J.-Y. Park and S.-M. Park, *Sensors*, 2009, **9**, 9513–9532.
7 N. Bangruwa and D. Mishra, *et al.*, *Sens. Actuators, B*, 2023, **382**, 133447.
8 N. Bangruwa, M. Srivastava and D. Mishra, *ACS Omega*, 2022, **7**, 37705–37713.

9 P. K. Bhartiya, Suryansh, N. Bangruwa, M. Srivastava and D. Mishra, *Anal. Chem.*, 2023, **95**, 3656–3665.
10 N. Bangruwa, M. Tiwari, A. Shandilya, R. Gutierrez, M. Peralta, S. Varela, G. Cuniberti and D. Mishra, *J. Phys. Chem. Lett.*, 2024, **15**, 2384–2391.
11 B. Göhler, V. Hamelbeck, T. Markus, M. Kettner, G. Hanne, Z. Vager, R. Naaman and H. Zacharias, *Science*, 2011, **331**, 894–897.
12 R. Naaman, Y. Paltiel and D. H. Waldeck, *Nat. Rev. Chem.*, 2019, **3**, 250–260.
13 D. Mishra, T. Z. Markus, R. Naaman, M. Kettner, B. Göhler, H. Zacharias, N. Friedman, M. Sheves and C. Fontanesi, *Proc. Natl. Acad. Sci. U. S. A.*, 2013, **110**, 14872–14876.
14 R. Torres-Cavanillas, G. Escorcia-Ariza, I. Brotons-Alcázar, R. Sanchis-Gual, P. C. Mondal, L. E. Rosaleny, S. Giménez-Santamarina, M. Sessolo, M. Galbiati and S. Tatay, *et al.*, *J. Am. Chem. Soc.*, 2020, **142**, 17572–17580.
15 N. Bangruwa, S. Suryansh, M. Peralta, R. Gutierrez, G. Cuniberti and D. Mishra, *J. Chem. Phys.*, 2023, **159**, 044702.
16 N. Bangruwa, M. Srivastava and D. Mishra, *Magnetochemistry*, 2021, **7**, 98.
17 I. V. Lightcap and P. V. Kamat, *J. Am. Chem. Soc.*, 2012, **134**, 7109–7116.
18 R. Ulbrich, *Solid-State Electron.*, 1978, **21**, 51–59.
19 M. Wöhlecke and G. Borstel, *Phys. Rev. B: Condens. Matter Mater. Phys.*, 1981, **23**, 980.
20 D. Pescia and F. Meier, *Surf. Sci.*, 1982, **117**, 302–309.
21 J. M. Abendroth, D. M. Stemer, B. P. Bloom, P. Roy, R. Naaman, D. H. Waldeck, P. S. Weiss and P. C. Mondal, *ACS Nano*, 2019, **13**, 4928–4946.
22 K. Ray, S. Ananthavel, D. Waldeck and R. Naaman, *Science*, 1999, **283**, 814–816.
23 Y. Zhang, G. Wu, W. Zhu, Z. Ji, Q. Jin and Z. Zhang, *Phys. Chem. Chem. Phys.*, 2021, **23**, 12612–12619.
24 S. Husain, S. Akansel, A. Kumar, P. Svedlindh and S. Chaudhary, *Sci. Rep.*, 2016, **6**, 28692.
25 M. Banyay, M. Sarkar and A. Gräslund, *Biophys. Chem.*, 2003, **104**, 477–488.
26 G. L. Long and J. D. Winefordner, *Anal. Chem.*, 1983, **55**, 712A–724A.
27 J. Prakash, A. Dey, S. Uppal, R. Alexander, A. Kaushal, H. S. Misra and K. Dasgupta, *Biosens. Bioelectron.*, 2021, **191**, 113480.